Human Molecular Genetics, 2019, Vol. 29, No. 4 566–579

doi: 10.1093/hmg/ddz270
Advance Access Publication Date: 9 December 2019
General Article

GENERAL ARTICLE

Functional genomics and gene-environment interaction highlight the complexity of congenital heart disease caused by Notch pathway variants

Gavin Chapman[1,2,*,†], Julie L.M. Moreau[1,§], Eddie Ip[1,‡,‖], Justin O. Szot[1,‖], Kavitha R. Iyer[1], Hongjun Shi[1,3], Michelle X. Yam[1], Victoria C. O'Reilly[1], Annabelle Enriquez[1,2,4,5], Joelene A. Greasby[1], Dimuthu Alankarage[1], Ella M.M.A. Martin[1], Bernadette C. Hanna[6], Matthew Edwards[6,7], Steven Monger[1], Gillian M. Blue[1,8,9], David S. Winlaw[1,8,9], Helen E. Ritchie[10], Stuart M. Grieve[11,12], Eleni Giannoulatou[1,13,‖], Duncan B. Sparrow[14,‖] and Sally L. Dunwoodie[1,2,13,¶]

[1]Victor Chang Cardiac Research Institute, Sydney, NSW, 2010, Australia, [2]Faculty of Medicine, University of New South Wales, Sydney, NSW, 2052, Australia, [3]Institute for Basic Medical Sciences, Westlake University, Hangzhou, China, [4]Department of Clinical Genetics, The Children's Hospital at Westmead, Sydney, NSW, 2145, Australia, [5]Discipline of Genomic Medicine, Faculty of Medicine and Health, University of Sydney, Sydney, NSW, 2006, Australia, [6]Hunter Genetics, John Hunter Hospital, Newcastle, NSW, 2298, Australia, [7]Department of Paediatrics, School of Medicine, Western Sydney University, Sydney, NSW, 2560, Australia, [8]Kids Heart Research, Heart Centre for Children, The Children's Hospital at Westmead, Sydney, NSW, 2145, Australia, [9]Sydney Medical School, University of Sydney, Sydney, NSW, 2006, Australia, [10]School of Medical Sciences, Faculty of Medicine and Health, University of Sydney, Sydney, NSW, 2006, Australia, [11]Sydney Translational Imaging Laboratory, Sydney Medical School, University of Sydney, Sydney, NSW, 2006, Australia, [12]Department of Radiology, Royal Prince Alfred Hospital, Sydney, NSW, 2050, Australia, [13]Faculty of Science, University of New South Wales, Sydney, NSW, 2052, Australia and [14]Department of Physiology, Anatomy and Genetics, University of Oxford, Oxford OX1 3PT, United Kingdom

*To whom correspondence should be addressed. Tel: +61 292958630, Fax: +61 292958601; Email: g.chapman@victorchang.edu.au.

Abstract

Congenital heart disease (CHD) is the most common birth defect and brings with it significant mortality and morbidity. The application of exome and genome sequencing has greatly improved the rate of genetic diagnosis for CHD but the cause in the majority of cases remains uncertain. It is clear that genetics, as well as environmental influences, play roles in the

[†]Gavin Chapman, http://orcid.org/0000-0002-3513-723X
[‡]Eddie Ip, http://orcid.org/0000-0002-4767-7583
[¶]Sally L. Dunwoodie, https://orcid.org/0000-0002-2069-7349
[‖]Authors contributed equally to the work.
[§]Present address: Development and Stem Cells Program, Monash Biomedicine Discovery Institute, Department of Anatomy and Developmental Biology, Monash University, Clayton, Victoria 3800, Australia.
Received: June 27, 2019. **Revised:** October 5, 2019. **Accepted:** November 4, 2019

aetiology of CHD. Here we address both these aspects of causation with respect to the Notch signalling pathway. In our CHD cohort, variants in core Notch pathway genes account for 20% of those that cause disease, a rate that did not increase with the inclusion of genes of the broader Notch pathway and its regulators. This is reinforced by case-control burden analysis where variants in Notch pathway genes are enriched in CHD patients. This enrichment is due to variation in *NOTCH1*. Functional analysis of some novel missense *NOTCH1* and *DLL4* variants in cultured cells demonstrate reduced signalling activity, allowing variant reclassification. Although loss-of-function variants in *DLL4* are known to cause Adams-Oliver syndrome, this is the first report of a hypomorphic *DLL4* allele as a cause of isolated CHD. Finally, we demonstrate a gene-environment interaction in mouse embryos between *Notch1* heterozygosity and low oxygen- or anti-arrhythmic drug-induced gestational hypoxia, resulting in an increased incidence of heart defects. This implies that exposure to environmental insults such as hypoxia could explain variable expressivity and penetrance of observed CHD in families carrying Notch pathway variants.

Introduction

Congenital heart disease (CHD) is the most common inborn malformation, affecting 0.8% of live births (1). Studies of familial recurrence have elucidated a significant genetic component to disease aetiology (2), with up to a third of cases receiving a clinically actionable genetic diagnosis (3). However, due to inconsistencies in penetrance and heterogeneity of CHD phenotype (expressivity), clinical genetic diagnoses in CHD cases can be fraught with uncertainty. This variability, and a proportion of the unexplained CHD cases, may be attributed to complex synergies of genetic and non-genetic factors.

Notch is an evolutionarily conserved signalling pathway that acts between cells in contact. Signalling is unidirectional from Delta, Serrate, and Lag 2 (DSL) ligands expressed on the surface of signal-sending cells to receiving-cells that express Notch receptors on their surface (4). Notch signalling influences cell proliferation, differentiation, cell fate decisions, and morphogenic events such as epithelial–mesenchymal transition, boundary formation, and lateral inhibition during embryonic development (5). Therefore, Notch signalling is crucial for the proper development of many embryonic structures and organs, including the vasculature and the heart (6). Heart development is regulated by Notch signalling in many ways including heart field specification, heart looping, and development of the atrioventricular canal, valves, myocardial trabeculae, outflow tract, coronary vessel, and atrioventricular node (7).

Given the crucial roles Notch signalling plays in heart development, it is not surprising that mutations in pathway components can lead to CHD. Variants in *NOTCH1* have been identified as a cause of sporadic or inherited human CHD (8–12). Importantly, these studies have shown that *NOTCH1* variants cause left- or right-sided heart lesions, are frequently inherited from asymptomatic parents, and the same variant may cause either isolated or syndromic CHD. CHD can also be caused by variants in other Notch pathway genes. Mutations in *MIB1*, encoding an ubiquitin ligase that alters Notch signal induction, may cause either isolated CHD (13) or left ventricular noncompaction cardiomyopathy (14). Mutations in Notch pathway genes are also associated with syndromes that can include CHD. For example, mutation of the genes encoding NOTCH2 and its cognate ligand JAG1 cause Alagille syndrome, in which CHD is present in almost all cases and varies from minor valve defects to major structural malformations. Additionally, mutations in *RBPJ*, *NOTCH1*, *DLL4*, and *EOGT* also cause Adams-Oliver syndrome (AOS) with or without associated heart defects, accentuating the importance of coordinated Notch signalling for normal development (15).

Notch pathway-associated CHD is characterised by variable penetrance and expressivity, likely caused by interaction with genetic and/or environmental factors. We have shown that short-term exposure of wildtype mice to hypoxia during gestation causes heart defects in about half the embryos (16). Moreover, gestational hypoxia also induces vertebral defects in mouse embryos. Here hypoxia inhibits fibroblast growth factor (FGF) signalling, halting cyclic NOTCH1 activation in the presomitic mesoderm and disrupting somitogenesis (17). Importantly, heterozygosity for Notch pathway components, including *Notch1*, interacts with hypoxia to increase the severity and incidence of vertebral defects in mouse embryos (17). Thus, Notch pathway genes, including *Notch1* itself, are excellent genetic candidates to study non-genetic influences on CHD phenotype variability.

Here, we have taken a multi-disciplinary approach to further explore the role of the Notch signalling pathway in the causation of CHD. This encompassed genome sequencing of families with CHD, functional genomic analysis of identified DNA variants, and exploration of gene-environment interaction in mice.

Results

Analysis of Notch pathway genes identifies significant burden of *NOTCH1* variation in CHD

Variants in several Notch pathway components have been implicated in syndromic or isolated CHD (18). Recently we conducted a family-based approach and identified clinically actionable monogenic causes of CHD in 10% of 30 families following whole exome sequencing and 31% of 97 families following whole genome sequencing (WGS) (3,19). Although all patients had severe CHD requiring surgery, they were not otherwise stratified by type of CHD, or whether it was familial or sporadic (Supplementary Material, Table S1).

Firstly, we investigated if variants in Notch pathway genes were enriched in our cohort of whole genome sequenced patients. We curated a list of 118 Notch pathway genes of which 33 were further defined as core genes essential for Notch signal transduction (Supplementary Material, Table S2). To determine if these genes are enriched for rare predicted-damaging variants, variant burden analyses were performed on 68 genome-sequenced probands with CHD (3) and 1127 control samples from the Medical Genome Reference Bank (MGRB) (20) that passed principal component analysis and missingness quality controls (Supplementary Material, Fig. S1). There was a significant enrichment of damaging variants with MAF <0.01 or <0.001 in the full list of 118 Notch pathway genes (Table 1). Focussing on 33 genes representing the core Notch pathway showed a significant enrichment in novel damaging variants as well as those with MAF <0.01 or <0.001. Although up to 34 damaging variants were identified through burden testing, the significant difference between CHD patients and controls was solely due to variants in *NOTCH1* (Table 1).

Table 1. Gene set analysis of Notch pathway genes

Gene set	ExAC MAF					
	Novel		<0.001 (0.1%)		<0.01 (1%)	
	P-value	Adjusted *P*-value	*P*-value	Adjusted *P*-value	*P*-value	Adjusted *P*-value
Notch core (33 genes)	0.00294	0.01761	0.01471	0.08828	0.02508	0.15045
Notch and regulators (118 genes)	0.27698	1	0.01118	0.06706	0.00966	0.05796
NOTCH1	0.00034	0.00206	0.00005	0.00032	0.00005	0.00032
Notch core excluding *NOTCH1* (32 genes)	0.15954	0.95723	0.50648	1	0.59400	1
Notch and regulators excluding *NOTCH1* (117 genes)	0.84909	1	0.10942	0.65653	0.08809	0.52852
Notch and regulators excluding Notch core (85 genes)	0.35533	1	0.11448	0.68688	0.07784	0.46705

Enrichment test *P*-values for novel and rare (MAF <0.001; MAF <0.01) variants from Notch pathway candidate gene sets. *P*-values represent the relative enrichment between cases (68 samples) and control (1127 samples). *P*-values were adjusted following Bonferroni correction for multiple comparisons. SNP-seq (Sequence) Kernel Association Test-Optimised (SKATO) was used for enrichment testing. Variant types selected for gene enrichment include stop gain, splicing, frameshift (insertion/deletion), nonsynonymous SNV. Only variants with deleterious scores for five predictors: SIFT, PolyPhen-2 HDIV, PolyPhen-2 HVAR, LRT and MutationTaster were included.

We further explored Notch pathway variation in our entire CHD dataset by aggregating all our genome and exome data and filtering for variants in Notch pathway genes using less stringent pathogenicity predictors than previously (see methods, 3,19). Of 114 analysed families, 51 (44%) had rare (MAF <0.01), predicted-damaging, protein-coding Notch pathway variants classified as pathogenic, likely pathogenic, or variant of uncertain significance (VUS) according to ACMG-AMP guidelines (Supplementary Material, Table S3). Of these, five variants in *NOTCH1* or *JAG1* were previously classified as pathogenic (Table 2) (3). 18/114 (16%) families carried a copy number variant (CNV) in a Notch pathway gene that overlapped genic or regulatory regions (Supplementary Material, Table S4). However, only one of these deleted coding exons of *NOTCH1* and therefore was considered pathogenic (Table 2) (3). This reanalysis identified a considerable number of variants in Notch pathway genes that were classified as VUS, largely because they are missense variants and in genes not recognised to cause CHD. It is possible that some cause CHD or contribute to disease. Additional functional analysis may provide evidence that such variants cause CHD.

Functional analysis allows a *DLL4* VUS to be reclassified as likely pathogenic

One of the novel variants we discovered in a core Notch pathway gene was in *DLL4* (c.763C>T p.P255S). In this family, the variant carriers (Family 3769, proband and father) had tetralogy of Fallot (TOF). Mutations in this gene have been associated with AOS (15,21). After identification of the familial *DLL4* variant, clinical examination revealed a small vascular lesion on the upper arm of the proband, but no other typical extra-cardiac features associated with AOS in either the proband or father, such as other vascular lesions, cutis aplasia, or transverse terminal limb defects. This variant did not pass *in silico* pathogenicity thresholds and was initially classified as a VUS. However, confirmation of this variant in another sibling, also born with isolated TOF (Supplementary Material, Fig. S2), suggested that the P255S variant might be sufficiently deleterious to protein function to cause this heart-specific phenotype.

To assess if the P255S variant alters the ability of DLL4 to activate NOTCH1, we performed co-culture assays that report on ligand-induced NOTCH1 signalling activity using cell lines stably expressing wildtype *DLL4* or the *DLL4* variant. Since our established assay used mouse cDNAs and cell lines (22,23), we created a P256S mutation in mouse *Dll4* that corresponds to P255S in human *DLL4*. Co-culture of wildtype DLL4-expressing cells with NOTCH1-overexpressing cells induced 68-fold activation of the Notch reporter when compared with control cell co-culture (Fig. 1A). P256S DLL4 was only able to activate NOTCH1 signalling with one-third the efficiency of the wildtype ligand (Fig. 1A, 23-fold induction). The subcellular localisation of P256S DLL4 to perinuclear vesicles and the plasma membrane was indistinguishable from wildtype DLL4 (Fig. 1B). P256S DLL4 was expressed at similar levels as the wildtype ligand in total protein lysates (Fig. 1C) as well as on the cell surface (Fig. 1D). Thus, despite the fact that P256S DLL4 is presented on the cell surface, its ability to activate NOTCH1 is significantly lower than wildtype. Therefore, the *DLL4* c.763C>T p.P255S variant was reclassified as likely pathogenic [LP (II)], a clinically actionable finding.

A novel variant in the LNR-A domain of the NOTCH1 receptor abrogates S1-processing and Notch signalling

We next chose two novel *NOTCH1* missense variants for functional assessment. The first variant (c.4416C>G p.C1472W, Family 152 900 216, Supplementary Material, Fig. S3A), initially classified as likely pathogenic (3), was chosen for functional assessment because it is the first to involve a cysteine in the LIN-12/NOTCH repeat (LNR)-A domain, a domain not previously associated with pathogenic CHD variants. The three LNR domains of Notch prevent metalloprotease cleavage in the absence of ligand binding and hence inappropriate activation of the receptor (24–26). The C1472W variant disrupts a disulfide bond that could result in constitutive receptor activity, as this disulfide bond and two others hold together the LNR-A domain in the absence of ligand binding. The second variant (c.2153A>G p.N718S, Family 1285, Supplementary Material, Fig. S3B) in EGF repeat 19 did not pass *in silico* pathogenicity thresholds (Supplementary Material, Table S3), and was classified as a VUS. However, it received a CADD Phred score of 18.92, so we hypothesised that this variant was also likely to have an effect on NOTCH1 protein function.

We performed co-culture assays that report on ligand-induced NOTCH1 signalling activity as above. Co-culture of cells expressing the ligand DLL1- or JAG1 with wildtype *Notch1*-transfected cells resulted in a 16- and 19-fold increase in reporter activity, respectively. N718S NOTCH1 similarly induced reporter activity (14- and 12-fold, respectively) and was not significantly

Table 2. Clinically actionable variants identified in Notch pathway genes

Family ID	Gene	Model	Familial CHD	ECA	Nucleotide variant	Amino acid variant	ExAC MAF	PP2 HVAR	CADD	ACMG Class	Cardiac Lesion
2831[a]	*NOTCH1*	AD[b]	Y	N	NM_017617.4: c.6105del	A2036Pfs∗3	0	–	22.7	P (Ic)	MOT
1852[a]	*NOTCH1*	AD[b]	Y	Y	NM_017617.4: c.5865del	N1955Kfs∗26	0	–	36	P (Id)	FSV
152900216[a]	*NOTCH1*	AD	Y	Y	NM_017617.4: c.4416C>G	C1472W	0	1	24.4	P (IIIb)[c]	MOT
169036865[a]	*JAG1*	AD	Y	Y	NM_000214.2: c.662G>C	G208R	0	0.999	32	P (IIIb)	MOT
3648[a]	*JAG1*	AD[b]	N	Y	NM_000214.2: c.2429C>T	P810L	8.32E − 06	0.955	34	P (II)	AVSD+
3769	*DLL4*	AD	Y	N	NM_019074.3: c.763C>T	P255S	0	0.182	23.2	LP (II)[c]	MOT
3173	*NOTCH1*	AD[b]	Y	Y	chr9:136537696-136560250del	Deletion of protein-coding exons 1 and 2	0	NA	NA	P	SDMA

Variants are present in all affected individuals within respective families. Chromosome positions are relative to hg38. Model, inheritance model; AD, autosomal dominant; Familial CHD, refers to the presence or absence of an individual with CHD within the immediate family of the proband; ECA, Extra-cardiac anomalies (not restricted to congenital defects); ExAC MAF, minor allele frequency in the ExAC database; NA, not applicable; PP2 HVAR, PolyPhen-2 HVAR predictive score. Score ≥ 0.909: probably damaging; 0.908 ≥ score ≥ 0.447: possibly damaging; score ≤ 0.446: benign. CADD: scaled CADD score ≥ 15: damaging. ACMG class: pathogenicity interpretation according to the ACMG-AMP guidelines: P, pathogenic; LP, likely pathogenic. Cardiac lesion: primary cardiac lesion of the proband. AVSD+, atrioventricular septal defect and variants; FSV, functional single ventricle; MOT, malformation of the outflow tract.

[a]Variant previously reported as the cause of CHD (3).

[b]Incomplete penetrance/variant present in unaffected individual.

[c]Variants which have been reclassified based on additional support from *in vitro* variant experimentation in this study (see Figs 1 and 2).

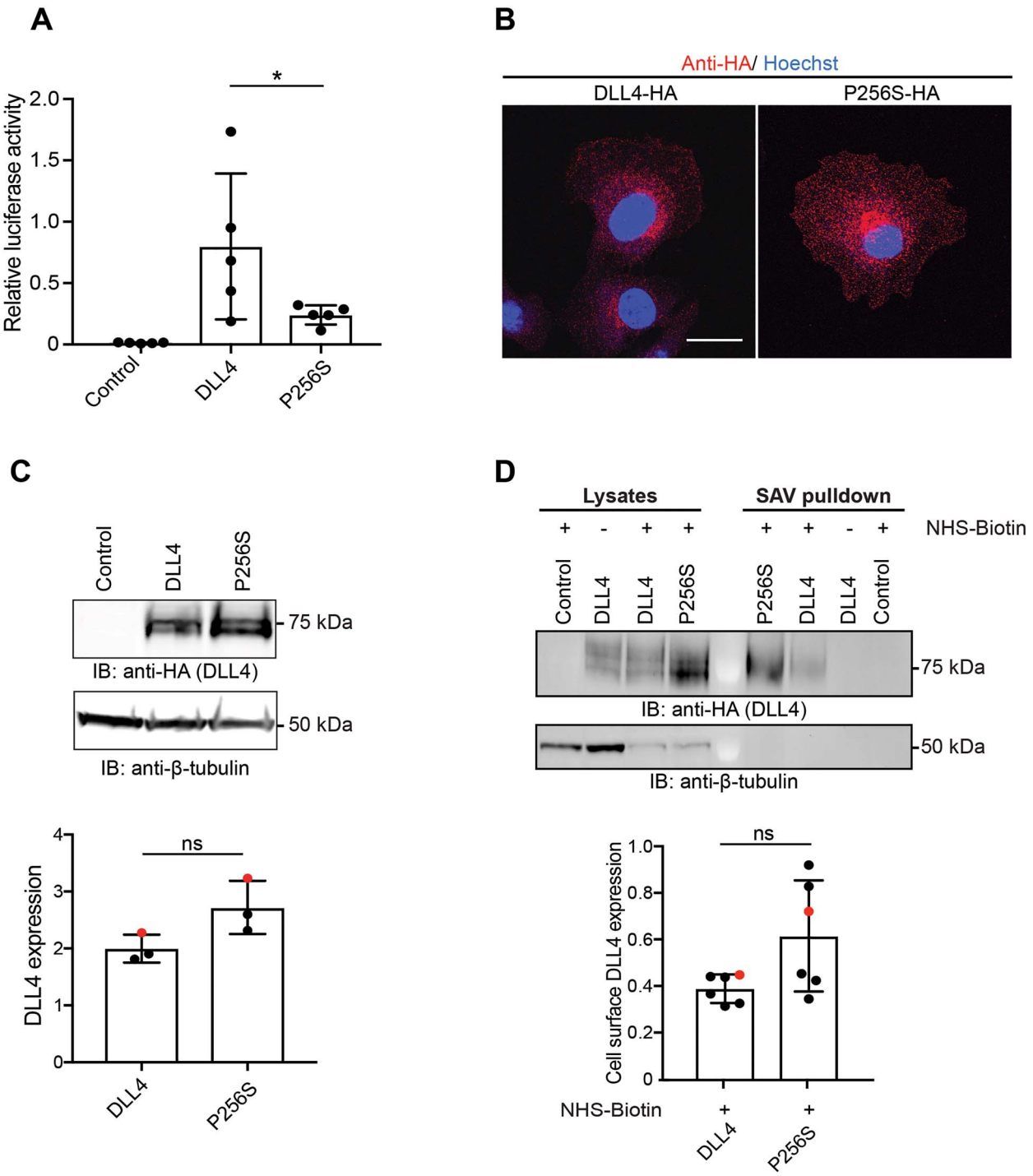

Figure 1. The P256S variant impairs DLL4-mediated Notch1 signalling in cells. **(A)** P256S DLL4 impairs Notch signalling in cells. C2C12 Notch1-FLAG cells transfected with Notch responsive reporter and co-cultured with WT (DLL4)-expressing, P256S DLL4-expressing cells or parental cells (control). Columns represent luciferase activity and s.d. of five independent experiments. *P = 0.0351. **(B)** Subcellular localisation of DLL4 in C2C12 LacZeo cells stably expressing WT and P256S DLL4. HA-tagged WT (DLL4-HA) and P256S DLL4 were detected with anti-HA and RRX. Nuclei are stained with Hoechst 33342. Scale bar = 20 μm. **(C)** Immunoblot showing WT and P256S DLL4 (anti-HA) expression in C2C12 LacZeo cells. Quantification of DLL4 expression is represented as normalised to β-tubulin. Error bars represent s.d. from three separate experiments. ns = not significant. The representative immunoblot is highlighted in red on the graph. **(D)** Cell surface presentation of WT and P256S DLL4. Detection of cell surface WT DLL4 and P256S DLL4 in C2C12 LacZeo cells. Cells were treated with sulfo-NHS-SS-biotin and cell surface proteins were pulled down with streptavidin beads from lysates and immunoblotted to detect DLL4 (anti-HA) and β-tubulin. Cell surface DLL4 expression is represented as a ratio of cell surface DLL4 levels normalised to respective input. Error bars represent s.d. from six independent experiments.

different from wildtype NOTCH1 (Fig. 2A). By contrast, C1472W NOTCH1 had limited signalling capacity, exhibiting only 2-fold higher reporter activity than untransfected cells (Fig. 2A). Immunofluorescence revealed that C1472W NOTCH1 lacked punctate vesicular and cell surface staining observed in wildtype NOTCH1 and N718S NOTCH1 (Fig. 2B). In total cell lysates,

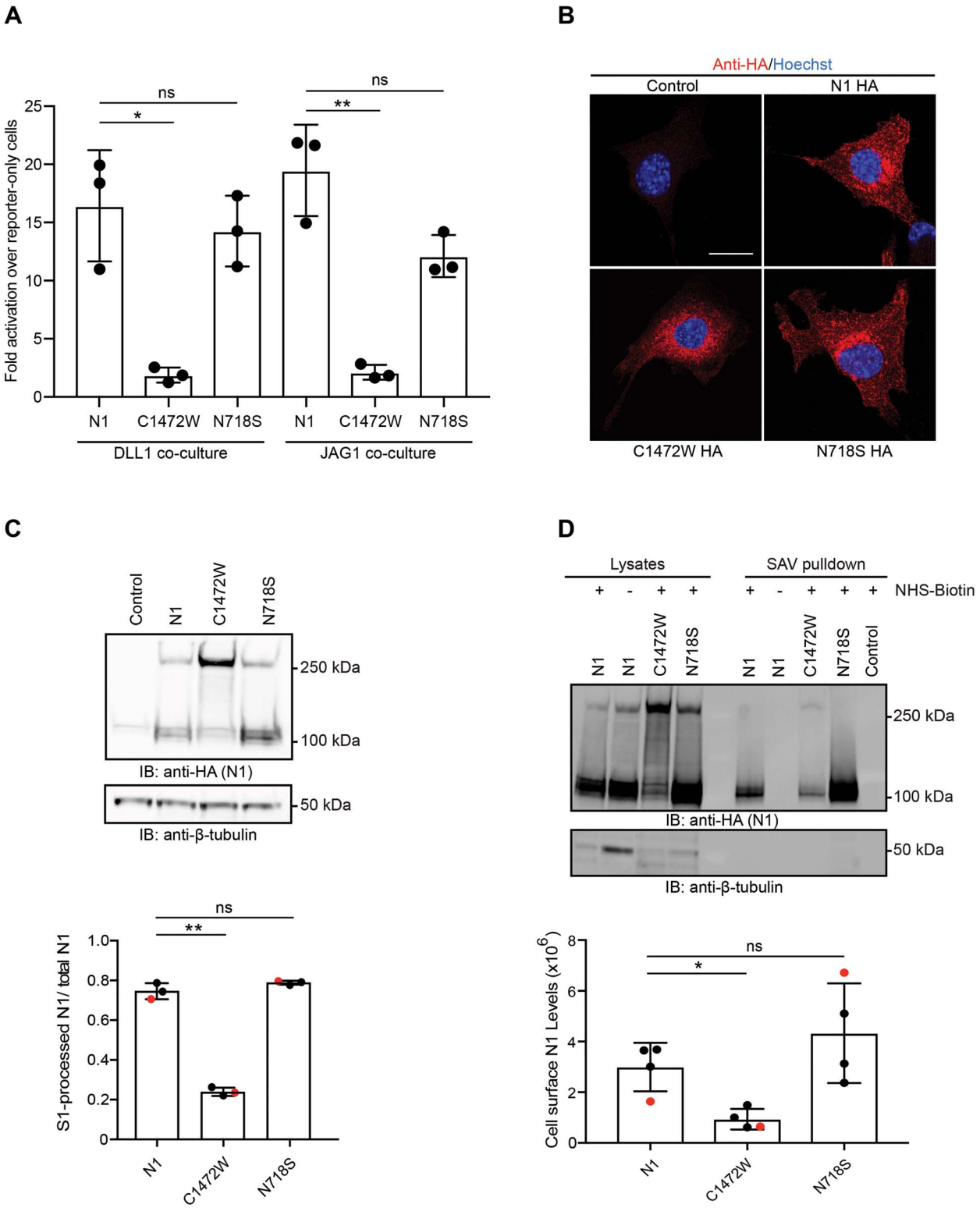

Figure 2. C1472W NOTCH1 lacks signalling capacity due to failed S1-processing. (**A**) Notch reporter activity upon co-culture with DLL1- or JAG1-expressing cells. NIH3T3 cells transfected with WT *Notch1*-HA (N1) and *Notch1*-HA carrying C1472W or N718S variants, and Notch reporter, were co-cultured with DLL1- or JAG1-expressing cells. Luciferase activity is represented as fold activation over cells transfected with reporter but not *Notch1*. Error bars represent s.d. from three independent experiments. $^{*}P = 0.0187$, $^{**}P = 0.0033$, ns = not significant. (**B**) Subcellular localisation of C2C12 cells stably expressing C1472W and N718S NOTCH1-HA (red) compared with WT NOTCH1-HA (N1HA) and negative control (C2C12 LacZeo parental cells). Nuclei are stained with Hoechst 33342 (blue). Scale bar: 20 µm. (**C**) Western blot detection of WT (N1), C1472W and N718S NOTCH1-HA (anti-HA) in stably expressing C2C12 cells. Ratio of S1-processed NOTCH1 to total NOTCH1 is shown. Error bars represent s.d. from three independent experiments. $^{**}P = 0.0042$. (**D**) Detection of cell surface NOTCH1 in C2C12 cells stably expressing WT (N1), C1472W and N718S NOTCH1-HA. Cells were treated with sulfo-NHS-SS-biotin and cell surface proteins were pulled down with streptavidin beads from lysates and immunoblotted to detect NOTCH1 (anti-HA) and β-tubulin. Quantification of cell surface NOTCH1 levels. Error bars represent s.d. from four independent experiments. $^{*}P = 0.033$.

approximately 74% of wildtype NOTCH1 was S1-processed, similar to N718S NOTCH1 (79%), while only 24% of C1472W NOTCH1 was S1-processed. Thus, most of C1472W NOTCH1 in the cell lysates is unprocessed rather than the heterodimeric form (Fig. 2C). S1-processing of the NOTCH1 receptor forms the NOTCH1 heterodimer and is critical for proper cell surface presentation of the receptor and for potent signal transduction (27–30). Precipitation of biotinylated cell surface proteins confirmed that less C1472W NOTCH1 was found on the cell surface than wildtype and N718S NOTCH1 (Fig. 2D). Therefore, C1472W NOTCH1 fails to undergo proper receptor maturation and cell surface presentation necessary for signal transduction while receptor maturation and signalling are unaffected by the N718S variant.

Gestational hypoxia interacts with *Notch1* heterozygosity to increase the incidence of heart defects in mice

In our CHD cohort, 8/10 (80%) of *NOTCH1* variants were inherited from an unaffected parent (Supplementary Material, Table S3), including two pathogenic frameshift variants. Incomplete penetrance of pathogenic *NOTCH1* variants has been well-documented (9,10,12), and is suggestive of additional disease risk modifiers, sensitising a genetic predisposition to disease in some but not all variant carriers.

Previously we have demonstrated that gene-environment interactions (G × E) between Notch signalling pathway genes and gestational hypoxia affect vertebral formation (17). We have also shown heart defects can be induced in mouse embryos when their wildtype mothers are exposed to gestational hypoxia (16). To assess the influence of hypoxia on a genetic predisposition to CHD, we first established the incidence of heart defects at different levels of low oxygen exposure in wildtype mice (Supplementary Material, Fig. S4). We identified a threshold in the sensitivity of cardiogenesis to low oxygen exposure, with 8% oxygen just above the threshold, similar to our previous observations for somitogenesis (17). We mated *Notch1*$^{+/-}$ males to *Notch1*$^{+/+}$ females to generate litters with both *Notch1*$^{+/-}$ and *Notch1*$^{+/+}$ embryos, and exposed these females to 8% oxygen (mild hypoxia) for 8 h at E9.5 before returning them to normoxia. Embryonic heart morphology was analysed at E17.5. Control litters from the same crosses developed in normoxia throughout gestation. Mild hypoxic exposure induced a significantly higher incidence of defects in *Notch1*$^{+/-}$ embryos (13/27) compared to unexposed *Notch1*$^{+/-}$ (0/15), and exposed (1/29) and unexposed (0/17) wildtype (*Notch1*$^{+/+}$) embryos (Fig. 3A, Supplementary Material, Table S5). A range of defects were observed including ventricular septal defect (VSD), overriding aorta (OA), double outlet right ventricle (DORV), transposition of the great arteries (TGA), atrial septal defect (ASD), straddling overriding tricuspid valve (SOTV) and hypoplastic left heart (HLH). Thus, mild hypoxia significantly increased the incidence of heart defects in *Notch1*$^{+/-}$ embryos.

We repeated our G × E experiments using maternal administration of the class III anti-arrhythmic drug dofetilide which causes embryonic bradycardia and hypoxia in rat embryos (31). Pregnant wildtype mice carrying *Notch1*$^{+/+}$ and *Notch1*$^{+/-}$ embryos were dosed once with dofetilide by oral gavage on the morning of E9.5, and embryonic heart morphology analysed 8 days later at E17.5. Dofetilide exposure induced a significantly higher incidence of defects in *Notch1*$^{+/-}$ embryos (13/28) compared to untreated *Notch1*$^{+/-}$ (0/15), treated (3/32), and untreated (0/17) *Notch1*$^{+/+}$ embryos (Fig. 3A). Thus, maternal exposure to a class III anti-arrhythmic drug significantly increased the incidence of heart defects in genetically susceptible mouse embryos.

To determine the molecular mechanism by which the *Notch1*-hypoxia G × E occurs, we performed immunohistochemistry on *Notch1*$^{+/+}$ and *Notch1*$^{+/-}$ embryos, immediately following exposure to 8 h hypoxia (8% oxygen), detecting total NOTCH1, cleaved (activated) NOTCH1 and MECA-32, which marks the endocardium and vasculature (32,33). Hypoxia treatment did not alter total NOTCH1 expression (Fig. 3B–F). Total NOTCH1 levels were reduced in *Notch1*$^{+/-}$ embryos compared to wildtype embryos, irrespective of whether or not embryos were exposed to hypoxia (Fig. 3B–F). In contrast to total receptor levels, cleaved NOTCH1 levels were unaffected by genotype in unexposed embryos (Fig. 3G–K). However, cleaved NOTCH1 levels were significantly reduced in *Notch1*$^{+/-}$ embryos exposed to mild hypoxia when compared with hypoxia-exposed wildtype embryos (Fig. 3G–K).

Previously we showed that mid-gestation exposure of mice to severe hypoxia (5.5% oxygen) induces heart defects in 43% of wildtype embryos by E17.5. Furthermore, immediately after the hypoxic exposure, FGF signalling was significantly reduced in the mesoderm of the second heart field (16). Here we show that, under the same conditions, total NOTCH1 expression in the outflow tract and atrial chamber was not affected in wildtype embryos (Supplementary Material, Fig. S5A–D). By contrast, cleaved NOTCH1 was significantly reduced in the vascular endothelial cells of the second heart field and the pharyngeal arches, and the endocardial cells of the atrial chamber (Supplementary Material, Fig. S5E–O).

We also tested the effect of 8% oxygen exposure on p-ERK levels (as a measure of FGF signalling) in *Notch1*$^{+/+}$ and *Notch1*$^{+/-}$ embryos (Supplementary Material, Fig. S6). Although there was a trend towards lower p-ERK levels in the second heart field of hypoxia-exposed embryos compared to unexposed embryos, this difference was not significant. p-ERK levels were also equivalent in *Notch1*$^{+/+}$ and *Notch1*$^{+/-}$ embryos, irrespective of hypoxia exposure. This is in contrast to an average reduction of 85% in p-ERK levels following exposure to 5.5% oxygen (16).

Together these data show that NOTCH1 signalling is only impaired with the combination of mild hypoxia and *Notch1* heterozygosity. Thus, there is interaction between the genetic susceptibility toward abnormal heart formation and an environmental stress during gestation leading to an increased incidence of heart defects.

Discussion

In this study, we have confirmed and extended the understanding of the role that Notch signalling, and more specifically NOTCH1, plays in human CHD. Firstly, whole exome- and genome-sequenced CHD datasets (3,19) were interrogated for variants in Notch signalling pathway genes and burden testing revealed an increased number of predicted damaging variants in *NOTCH1* and in Notch pathway genes in our CHD cohort compared to controls. Next, selected missense variants were tested functionally, revealing that a variant in *DLL4* and a variant in the unexplored LNR-A domain of *NOTCH1* can cause isolated CHD and CHD with extra-cardiac anomalies, respectively. Variants in core Notch pathway genes accounted for 20% of identified causative variants in our WGS cohort (3). Finally, we demonstrate using two means of inducing hypoxia in embryos

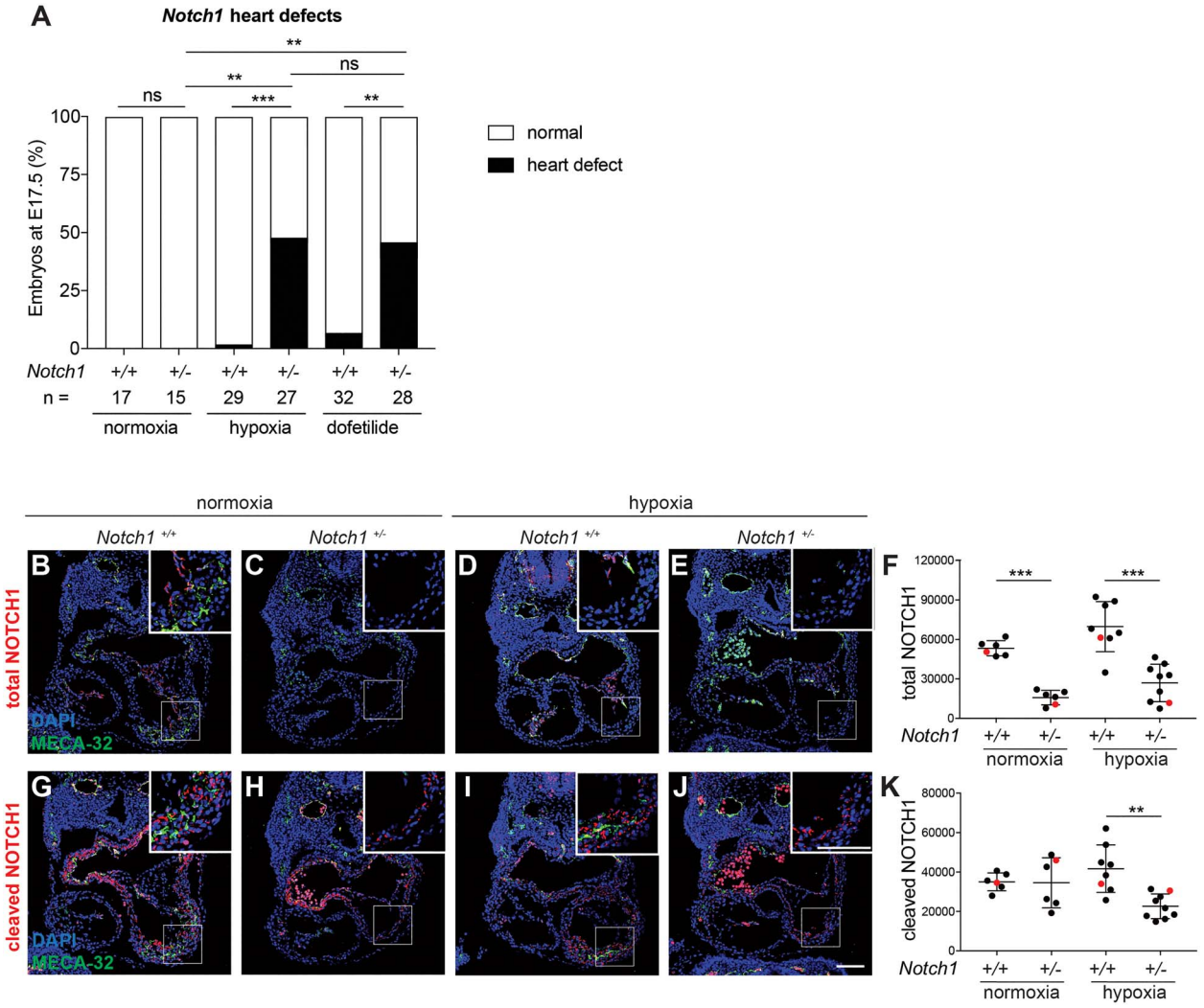

Figure 3. Exposure to environmental teratogens increases the incidence of heart defects in *Notch1*$^{+/-}$ mouse embryos. (**A**) The heart morphology of mouse embryos exposed to 8% Oxygen (hypoxia) or gavaged with 2 mg/kg of dofetilide at E9.5 and assessed at E17.5. The graph represents the percentage of embryos with normal heart (white) and those with heart defects (black). See Supplementary Material, Table S5 for types of heart defects. (**B–E**) Representative paraffin heart sections immunostained with endothelial marker MECA-32 (green) and total NOTCH1 (red). Nuclei were stained with DAPI (blue). Insets in B–E are higher magnifications of the boxed areas. (**F**) Graph representing the total NOTCH1 staining intensity relative to MECA-32 area in the indicated genotypes and conditions. (**G–J**) Representative paraffin heart sections immunostained with MECA-32 (green) and cleaved NOTCH1 (red). Nuclei were stained with DAPI (blue). Insets in G–J are higher magnifications of the boxed areas. (**K**) Graph representing cleaved NOTCH1 staining intensity relative to MECA-32 area in the indicated genotypes and conditions. Data were tested for statistical significance by Fisher's exact test (A) and one way ANOVA (F, K). Error bars represent s.d. Red dots indicate quantification of the images shown in B–E and G–J. $^{**}P < 0.01$, $^{***}P < 0.001$. scale bars: 100 µm in B–E and G–J.

that each interacts with *Notch1* heterozygosity to increase the incidence of heart defects in mice.

NOTCH1 variants have been reported as candidates for causing cases of isolated CHD (3,8,10,19) and an increased burden of Notch pathway variation has been identified in patient cohorts (11,34). We report here that damaging variation in Notch pathway genes is enriched in our cohort of CHD patients, which constitutes a broad range of CHD phenotypes requiring surgical correction. This is consistent with the observation that variants in core Notch pathway genes account for 20% of identified causative variants in our WGS cohort (3). We conclude however that this is due to variants in *NOTCH1* as enrichment is lost when *NOTCH1* variants are removed, and because *NOTCH1* variants alone are significantly enriched in our CHD probands compared with controls. Consistent with this, of the seven pathogenic or likely pathogenic Notch pathway variants identified, four occur in *NOTCH1*. In summary, our data further demonstrates that Notch pathway variation is enriched in CHD patients, and we extend the importance of the Notch pathway by uniquely applying the ACMG-AMP variant classification to demonstrate the pathogenic/likely pathogenic nature of these clinically actionable variants.

We identified a pathogenic missense variant in *JAG1* (c.662G>C p.G208R) in a proband with malformation of the outflow tract (Family 169 036 865). The proband's father and three siblings, all with various types of CHD, also carried this *JAG1* variant. The proband was not initially suspected of having Alagille Syndrome, as the typical diagnostic features of the syndrome were not evident. However, further investigation informed by this *JAG1* variant revealed corneal, vascular and liver anomalies leading to a diagnosis of Alagille Syndrome in this family. Notably, the molecular diagnosis in one relative

(181678920) prompted neurological investigations of stroke-like episodes and a diagnosis of Moyamoya syndrome successfully treated with encephaloduroarteriomyosynangiosis. Thus, the genetic diagnosis has potential to enhance the family's clinical care (Supplementary Material, Fig. S7).

We identified a missense variant *DLL4* c.763C>T p.P255S in three individuals in the same family with TOF (Family 3769). Truncating variants and presumed loss-of-function missense variants in *DLL4* cause AOS, a rare congenital disease in which patients characteristically have aplasia cutis congenita of the scalp vertex and terminal transverse limb defects (15,21). CHD is present in 20% of AOS patients, typically TOF, VSD, and defects of the great arteries and their valves (35,36). The P255S variant impairs, but does not abolish, the ability of the DLL4 ligand to activate the NOTCH1 receptor. Cell surface levels of DLL4 are not affected by the P255S variant, suggesting that this variant and therefore EGF3 directly influences receptor activation. That a residue in EGF3 is important for receptor activation is consistent with observations that the MNNL-EGF3 region of DLL4 is required for receptor activation (37). While highest receptor affinity appears to require the N-terminus to EGF2 of DLL4, EGFs 3–5 also add to the overall affinity for the receptor (38). Thus, impaired Notch activation by DLL4 P255S is likely to be due to reduced affinity of this variant ligand for the NOTCH1 receptor. The variant introduces a serine residue necessary for glucosylation, the occurrence of which could alter receptor interaction, however the site in question (C1ISHNGC2, where C1 refers to the first cysteine of the EGF repeat) is not a close match to the POGLUT1 glucosyltransferase specific consensus (C1XSXPC2) (39).

Given that DLL4 P255S is hypomorphic in our Notch signalling assay, we were able to reclassify this variant according to ACMG-AMP guidelines, from VUS to likely pathogenic, a classification that is clinically actionable. This finding indicates that deleterious alleles in *DLL4* can cause isolated CHD as well as AOS. Most *DLL4* missense variants reported to cause AOS involve cysteines, disrupting the structure of the epidermal growth factor (EGF)-like repeat and presumably affecting protein trafficking and hence signalling activity (15,21,40,41). Of the remaining reported *DLL4* missense variants, some are thought to disrupt ligand-receptor interaction, although none have been functionally tested. We hypothesise that hypomorphic *DLL4* alleles cause isolated CHD, while missense variants that have a more severe effect on DLL4 function result in AOS. This could be tested by comparative functional analysis of previously reported AOS-causing missense *DLL4* variants (15,21,40,41).

We previously identified the *NOTCH1* variant c.4416C>G p.C1472W in a family (152900216) with DORV, pulmonary stenosis and VSD in the proband, and aortopulmonary window in the father, and both with digit anomalies (3). The C1472W variant removes a cysteine that forms a structural disulphide bond in the LNR-A domain. Gain-of-function mutations in the LNR domains have been associated with T-cell lymphoblastic leukaemia (T-ALL) although it is normally caused by mutations in the heterodimerisation (HD) and PEST domains (42). Indeed, disruption of the LNR-A domain may be predicted to activate the receptor without the need for ligand. In the absence of ligand co-culture, Notch reporter levels were comparable irrespective of whether the C1472W variant was present, indicating that the variant does not render NOTCH1 constitutively active (data not shown). Instead, the C1472W variant almost abolishes the receptor's ability to signal in response to ligand. Defective signalling via C1472W NOTCH1 is not due to a lack of receptor expression but rather a failure of S1-processing and consequent cell surface presentation. Thus, rather than constitutively activating the NOTCH1 receptor, the C1472W variant causes a block of receptor trafficking. This finding justifies reclassification of the C1472W *NOTCH1* variant from likely pathogenic to pathogenic. Recently, the proband was reported to have *cutis marmorata*, which, in addition to her CHD and terminal limb defects, is consistent with AOS caused by pathogenic *NOTCH1* mutations (43,44).

The *NOTCH1* variant c.2153A>G p.N718S has no effect on receptor signalling. We therefore explored if this variant might disrupt *NOTCH1* pre-mRNA splicing, as missense variants in *NOTCH1* that also alter *NOTCH1* pre-mRNA splicing can cause CHD (10). *NOTCH1* c.2153A>G received a MaxEntScan score (45) of 7.68 for creation of a donor motif within exon 13, 65 bp upstream of the endogenous exon 13 donor site and resulting in a frameshift. The endogenous exon 13 donor site has a similar score (7.73), indicating that the c.2153A>G variant may compete with the endogenous donor motif. It will be important to assess the effect of this variant on *NOTCH1* pre-mRNA splicing, if additional blood samples become available. Until then, *NOTCH1* c.2153A>G p.N718S remains a VUS.

The functional tests described here demonstrate abrogated protein function due to *DLL4* and *NOTCH1* variants found in CHD patients. While such functional assays improve the diagnostic rate, the improvement is modest and the assays very time consuming. The challenge with such functional genomics approaches in the future will be to efficiently test the consequences of multiple candidate variants in genes, the products of which have disparate or unknown molecular or biochemical functions.

It can be argued that heterozygous mutations in *NOTCH1* are the most common genetic cause of CHD and yet, as is the case with mutations in other genes, there is variable penetrance and expressivity of *NOTCH1* mutations even within families (10–12,34). We demonstrate a G × E between *Notch1* heterozygosity and exposure to mild hypoxia (8%) or dofetilide that leads to a substantial increase in the incidence of heart defects. Importantly, the defects in *Notch1*$^{+/-}$ embryos exposed to mild hypoxia include VSD, OA, DORV, HLH and SOTV. These defects are similar to heart phenotypes that have been observed in humans heterozygous for mutations in *NOTCH1* such as VSD, DORV, HLHS, TOF and dysmorphic aortic valve (8,9,34); and a 190 kb deletion including *NOTCH1* is also associated with TOF, VSD, OA, right ventricular hypertrophy and pulmonary stenosis (46). The close similarity in the types of heart defects present in *NOTCH1* variant heterozygous humans and *Notch1*$^{+/-}$ mice exposed to mild hypoxia suggests that similar G × E might be of clinical relevance.

In mice, only the combination of mild hypoxia and *Notch1* heterozygosity impairs NOTCH1 signalling, arguing against independent actions of the genetic and environmental factors on heart morphogenesis. *Notch1* heterozygotes express lower levels of receptor protein, but signalling is only reduced when combined with mild hypoxia. In wildtype mice, NOTCH1 signalling is only impaired under severe hypoxia, despite unchanged receptor expression. Together, these observations suggest that hypoxia disrupts Notch signalling *per se*. This could occur upstream or downstream of the receptor. Upstream, hypoxia might reduce the availability of DSL ligands by impeding their expression or maturation. Although we could not detect DLL4 and JAG1 protein reliably in embryonic heart sections, this hypothesis seems unlikely for two reasons. Firstly, more severe hypoxia does not affect the expression or subcellular localisation of DLL1 or DLL3 in the presomitic mesoderm of E9.5 mouse embryos (17). Secondly, hypoxia *induces* DLL4 expression in the vasculature (47). Hypoxia acting downstream of the NOTCH1 receptor also seems

unlikely, as hypoxia is reported to increase receptor activation by enhancing gamma-secretase cleavage of the receptor and by stabilising the cleaved/activated receptor (48). Thus, the mechanism by which NOTCH1 activation is reduced in our studies remains unexplained. Clearly however, cellular context, severity and extent of hypoxia, and assay design are all likely to affect the outcomes.

Other studies have found that environmental factors can also interact with the Notch pathway to cause heart defects and disease. For example, haemodynamic parameters worsen and calcific aortic disease is evident when *Rbpj* heterozygous mice are fed a hypercholesterolemic diet supplemented with vitamin D (49). Also, the incidence of ventricular septal defect is increased in *Notch1* heterozygous embryos upon induction of maternal hyperglycemia (50), an observation relevant to humans as pre-pregnancy diabetes mellitus significantly increases the chance that affected mothers will have a child with CHD (51,52). Our finding that embryonic exposure to hypoxia at E9.5, equivalent to 21–23 days post-fertilisation in humans, increases the rate of heart defects in *Notch1* heterozygous mouse embryos suggests that environmental factors, when coupled to genetic susceptibility, increase the incidence of heart defects in humans. There are many recognised maternal factors that reduce the oxygen supply to the embryo such as smoking, living at high altitude, diabetes, high body mass index, hypertension, and prescription medication use (53–59). We showed that maternal administration of dofetilide increases the rate of heart defects in *Notch1* heterozygous embryos. Dofetilide binds and disrupts hERG, which is the pore-forming subunit of the delayed rectifier voltage gated K+ channel, and affects cardiac contraction (60). Hundreds of currently prescribed medications (~10% of the total) have the potential to bind and disrupt hERG (https://crediblemeds.org/). If taken in the context of pregnancy, any of these might induce embryonic hypoxia which, in combination with a genetic predisposition, could cause CHD, alter the penetrance, or explain variable expressivity of CHD within or between families harbouring Notch pathway gene mutations.

In summary, the Notch signalling pathway is becoming increasingly associated with the genetic causation of CHD in humans. Our research strengthens this observation, and also provides a credible explanation for the phenotypic variability in families carrying deleterious variants in Notch pathway genes. Our results have immediate clinical implications. Many therapeutic drugs in common use have the side-effect of disrupting hERG channel activity and might be taken at a crucial time for heart development (3–4 weeks post fertilisation), which is often before a woman knows she is pregnant. We have shown that one such drug can exacerbate the effects of *Notch1* haploinsufficiency. Thus, use of such drugs peri-conceptionally should be reviewed in families with a history of CHD.

Materials and Methods

Study participants

Ethical approval for this study was obtained from the Sydney Children's Hospital Network Human Research Ethics Committee (approval number HREC/16/SCHN/73). The cohort consisted of 114 families of which 45 were recruited at Princess Margaret Hospital for Children (PMH), Perth, Australia, 60 from the Kids Heart Research DNA Bank based at The Children's Hospital at Westmead (CHW), Sydney, Australia, and nine via independent clinicians. Families from PMH and CHW were recruited at pre-admission clinics prior to cardiac surgery, and included both familial and sporadic CHD cases. Heart defects in all affected individuals ($n = 181$) were confirmed by echocardiography. Cardiac phenotypes of the 181 affected individuals were grouped into seven main categories (Supplementary Material, Table S1): atrioventricular septal defect (AVSD) and variants ($n = 9$), septal defect (excluding AVSD; $n = 47$), septal defect with minor cardiac anomalies ($n = 25$), malformation of the outflow tract ($n = 44$), obstructive lesion ($n = 15$), functional single ventricle ($n = 20$), and other ($n = 21$). Any clinical phenotype that was not a heart defect was referred to as an extra-cardiac anomaly (ECA). Study participants are further described in Refs. (3,19).

Rare variant enrichment analyses

Whole genome sequencing reads of 97 unrelated CHD probands (3) were aligned to the Human Reference Genome Hg19 using BWA v0.7.15 (61) and variants called with GATK v3.8 (62) to allow comparisons to be made to the Medical Genome Reference Bank (MGRB) cohort (20) used here as a controls. Principal Component Analysis (PCA) was performed to facilitate exclusion of ethnic outliers (Supplementary Material, Fig. S1A) (63), which reduced the case samples to 73 and control samples to 1127. Sample quality control metrics used for the MGRB study were applied to the cases samples, including sample missingness <1.5% filter (Supplementary Material, Fig. S1B), which further reduced the case samples to 68. For enrichment analysis, novel and rare variants (MAF <0.001 or <0.01) were included if they were considered disruptive (nonsense, frameshift and essential splice-site mutations) or missense variants rated as 'damaging' by all of five prediction algorithms employed (PolyPhen-2 HDIV and HVAR, LRT, MutationTaster and SIFT) as described previously (64). Enrichment analyses were performed on these variants sets using SNP-set (Sequence) Kernel Association Test-Optimised (SKAT-O) test (65) to determine association of mutation burden.

Variant filtration of whole exome and genome sequence data

Genomic variants from 17 unique whole exome and 97 whole genome-sequenced families with CHD were called, annotated, and quality-controlled previously (3,19). Variants in protein-coding regions of 118 genes associated with Notch signalling (Supplementary Material, Table S2) were then prioritised for pathogenicity using *in silico* and population frequency thresholds using in-house scripts as previously described (19). In exceptional cases, where only affected individuals per family harboured a predicted-damaging, novel variant with respect to healthy reference population databases, a minimum of two of three pathogenicity thresholds were required to be passed for variant consideration. Variants present in all affected individuals in a given family were then interpreted according to the standards and guidelines established by the American College of Medical Genetics and Genomics and Association for Molecular Pathology (ACMG-AMP) (66). A web-based tool, InterVar (67), was used to obtain an interpretive classification of the variants according to these guidelines. Copy number variants (CNVs) from genome sequence data overlapping these genes, or their regulatory regions, were interrogated as previously reported (3).

Gene specific primers were used to amplify genomic DNA surrounding each functionally tested variant (Supplementary Material, Table S6) using DreamTaq (Thermo Fisher) according to the manufacturer's instructions. Products were purified with either ExoSAP-IT (Thermo Fisher) or gel purification (Qiagen)

prior to Sanger Sequencing at Garvan Molecular Genetics (Darlinghurst, NSW, Australia) with primers listed in Supplementary Material, Table S6.

Mutagenesis, cloning and cell culture

Mutagenesis was carried out on mouse *Dll4* and *Notch1* cDNAs in pEntr2B (Thermo Fisher) according to the QuikChange method using Kapa HiFi polymerase (Kapa Biosystems) with primers listed in Supplementary Material, Table S6. C2C12 cells and NIH3T3 cells were cultured in DMEM containing 10% foetal calf serum in 10% CO_2. Wildtype (WT) and mutated *Dll4* and *Notch1* were gateway-cloned into pCMX-HA and pCDNA5-HA FRT/TO (68). C2C12 cell lines stably expressing wildtype (WT) and P256S-mutated DLL4 were generated using the Flp-In system (Thermo Fisher). Briefly, WT and P256S-mutated *Dll4* were gateway-cloned into the pCDNA5-HA FRT/TO plasmid (68) and then transfected along with the FRT expression plasmid pOG44 into C2C12 harbouring the LacZeo cassette. The cultures were passaged the next day and 110 µg/ml hygromycin B was added the following day. After 10 days, surviving colonies were pooled and transgene expression was confirmed by western blot and immunofluorescence detecting the HA-tag. Wildtype *Notch1* was gateway-cloned into pCAG-IRESpuro to generate pCAG-Notch1-FLAG-IRESpuro. C2C12 cells stably expressing mouse NOTCH1-FLAG were generated by transfecting cells with pCAG-Notch1-FLAG-IRESpuro. Cultures were grown in 1.5 µg/ml puromycin for 10 days, colonies picked and screened by immunofluorescence and immunoblotting for anti-FLAG reactivity.

Co-culture assays of Notch signal transduction were carried out as described in (23). To analyse *NOTCH1* variants, NIH3T3 cells were transfected with WT Notch1-HA pCMX or Notch1 carrying C1472W or N718S point mutations and the p6xTP1-Luc synthetic Notch reporter (68). After 5 h, the transfection medium was removed and replaced with medium containing JAG1-expressing cells, DLL1-expressing cells or control cells. To analyse the DLL4 P255S variant, C2C12 cells stably expressing FLAG-tagged NOTCH1 were transfected with the p6xTP1-Luc reporter and following transfection, were co-cultured with WT or P256S-mutated mouse DLL4-expressing cells or control cells overnight. The following day co-cultures were lysed and underwent luciferase assay on a PHERAstar *FS* plate reader. Relative luciferase units were calculated by dividing Firefly luciferase readings by Renilla luciferase readings and triplicate values were then averaged. The data were either graphed as relative luciferase units or as fold activation over control co-culture. Data were natural log-transformed and statistical significance established in Prism 8 software (GraphPad) using one-way ANOVA with Sidak multiple comparison correction.

Immunofluorescence

Immuno-cytochemistry was carried out using the gelatin-saponin method as described in (69) using rabbit anti-HA (1:1000, C29F4, Cell Signaling Technology) and Rhodamine Red-X conjugated anti-rabbit secondary (1:1000, Jackson ImmunoResearch) antibodies and Hoechst 33342 (1:100 000; Thermo Fisher). Images were acquired on an AxioObserver Z1 inverted microscope equipped with 710 scan head using a 63× 1.4 NA oil objective (Zeiss) or an Axioimager Z1 upright microscope equipped with 700 scan head using a 63× 1.4 NA oil objective (Zeiss).

For immuno-histochemistry, embryos were harvested at E9.5, fixed overnight in 4% paraformaldehyde at 4°C, embedded in paraffin and 10 µm sections were collected in the sagittal or transversal plane as described in (16). To minimise inter-slide staining variation, tissue arrays were made by placing six heart sections of 2–4 embryos on each slide. Antigen retrieval for all antibodies was performed using TE buffer as described in (70). The antibodies used are the following: rabbit anti-NOTCH1 (1:500, D1E11, Cell Signaling Technology), rabbit anti-cleaved NOTCH1 (1:400, Val1744 D3B8; Cell Signaling Technology) rat anti-Mouse Endothelial Cell Antigen 32 (1:20, MECA-32; DSHB). Donkey anti-rat Alexa-488 (1:1000, A21208, Molecular Probes), biotinylated donkey anti-rabbit (1:500, 711–065-152; Jackson ImmunoResearch) secondary and streptavidin Cy3 (1:1000, GTX85902; GeneTex) tertiary reagents were used to detect primary antibodies. Nuclei were stained with DAPI (1:1000, 0236276001; Merck) and slides mounted in Mowiol® with DABCO. Images were captured on AxioObserver Z1 upright microscope with a 700 scan head using a 10× objective (Zeiss). Staining intensity of immunohistochemistry on paraffin sections was quantified using ImageJ 1.48a (NIH, USA). Briefly, LSM files generated by confocal microscopy were imported into ImageJ. The region of interest was manually defined, and the optimum image threshold was determined for the staining of interest and nuclei. Identical threshold values were used for all images of each experiment. The signal of the protein of interest above threshold was quantified as a Raw Integrated Density and divided by the nuclei area from five to six independent sections from the same embryo. Data were found to be normally distributed by the Shapiro-Wilk normality test and therefore statistical significance determined using an ordinary one-way ANOVA with Tukey's post-hoc test.

Precipitation of cell surface proteins and immunoblotting

Cells were grown to 80–90% confluency, washed three times with ice-cold PBS containing 1 mM $MgCl_2$ and 0.1 mM $CaCl_2$ and cell surface proteins labelled with 1 mg/ml EZ-Link sulfo-NHS-SS-biotin (Pierce) in cold Biotin Buffer (154 mM NaCl, 10 mM HEPES, 3 mM KCl, 1 mM $MgCl_2$, 0.1 mM $CaCl_2$, 10 mM glucose, pH 7.6) and biotinylation was performed as described in Ref. (71). Immunoblotting was performed using the Bolt western blot system (Thermo Fisher) with anti-HA (1:1000; C29F4; Cell Signaling), and anti-β-tubulin (1:10 000; T5201; Sigma) primary antibodies and HRP (1:20 000; Jackson) secondary antibody. Immunoblots were scanned using the ChemiDoc MP Imaging system (Bio-Rad). Band intensities were quantified using Image lab (Bio-Rad). Data were natural log-transformed and statistical significance established in Prism 8 software (GraphPad) either by Student's t-test with Welch's correction or one-way ANOVA with Sidak multiple comparison correction.

Animal experiments

This research was performed following the guidelines, and with the approval, of the Garvan Institute of Medical Research/St. Vincent's Animal Experimentation Ethics Committee, research approvals 9/33, 12/33 and 15/27. The *Notch1* knockout allele was generated by crossing *Notch1* Flox [$Notch1^{tm2Rko}$] (72) to the CMV-Cre line. Male mice heterozygous for *Notch1* were crossed with C57BL/6 J wildtype females to produce heterozygous and wildtype embryos. Pregnant mice were exposed to reduced oxygen levels at normal atmospheric pressure as described (17). After exposure, the mice were either sacrificed and embryos harvested or returned to normoxia. For the dofetilide treatments, pregnant

females were administered with 2 mg/kg dofetilide by oral gavage (31) at E9.5.

Heart morphology determination

Heart morphology at E17.5 was determined as described previously, either by magnetic resonance imaging (MRI) and confirmed by histology (73) or by optical projection tomography (OPT) (16). Briefly, hearts were excised and fixed in 4% paraformaldehyde overnight at 4°C. Hearts were then dehydrated in methanol and finally cleared overnight in benzyl alcohol:benzyl benzoate (BABB). OPT scanning was performed using a custom built OPT microscope controlled by purpose-built software OPTiscan (James Springfield, Institute for Molecular Biosciences, University of Queensland, Australia). 800–1200 autofluorescence images in the FITC channel were collected per sample. These were reconstructed using NRecon (Bruker micro-CT, Belgium). Data were visualised in Amira (Thermo Fisher). E17.5 heart morphology was assessed by the same observer, with classification of heart defects confirmed by an independent assessor. Significance of differences in the incidence of induced heart defects in G × E experiments were tested using one-tailed Fisher's exact tests.

Supplementary Material

Supplementary Material is available at *HMG* online.

Acknowledgements

We thank R. Kopan for the *Notch1* Flox mouse line and B.E. Chapman, S. O'Donnell and M. Rapadas for technical assistance. We are grateful to the families who participated in this research, and individuals and agencies that supported this research. Forty-five and Up is managed by the Sax Institute in collaboration with major partners (see www.saxinstitute.org.au). The authors acknowledge the contributions from the investigators, staff, general practitioners and, in particular, the study participants, from the 45 and Up and ASPREE studies.

Funding

The MGRB was funded by the NSW State Government and is made up of data from the ASPREE and 45 and Up studies. Funding support for ASPREE and the ASPREE Healthy Ageing Biobank was from the NIH (National Institute on Aging and National Cancer Institute), Monash University, the CSIRO and the Victorian Cancer Agency. This work was supported by the National Health and Medical Research Council (NHMRC) Project grant APP1019776 to S.L.D., D.B.S. and S.M.G., Fellowships ID514900, ID1042002 to S.L.D., NSW Health Early-Mid Career Fellowship and the National Heart Foundation of Australia Future Leader Fellowship ID101204 to E.G. Key Foundation, Chain Reaction, and the Office of Health and Medical Research NSW Government to S.L.D.

Conflict of interest

The authors declare no conflicts of interest.

References

1. van der, D., Konings, E.E.M., Slager, M.A., Witsenburg, M., Helbing, W.A., Takkenberg, J.J.M. and Roos-Hesselink, J.W. (2011) Birth prevalence of congenital heart disease worldwide: a systematic review and meta-analysis. *J. Am. Coll. Cardiol.*, **58**, 2241–2247.
2. Akhirome, E., Walton, N.A., Nogee, J.M. and Jay, P.Y. (2017) The complex genetic basis of congenital heart defects. *Circ. J.*, **81**, 629–634.
3. Alankarage, D., Ip, E., Szot, J.O., Munro, J., Blue, G.M., Harrison, K., Cuny, H., Enriquez, A., Troup, M., Humphreys, D.T. *et al.* (2019) Identification of clinically actionable variants from genome sequencing of families with congenital heart disease. *Genet. Med.*, **21**, 1111–1120.
4. Bray, S.J. (2016) Notch signalling in context. *Nat. Rev. Mol. Cell Biol.*, **17**, 722–735.
5. Hansson, E.M., Lendahl, U. and Chapman, G. (2004) Notch signaling in development and disease. *Semin. Cancer. Biol.*, **14**, 320–328.
6. Siebel, C. and Lendahl, U. (2017) Notch Signaling in development, tissue homeostasis, and disease. *Physiol. Rev.*, **97**, 1235–1294.
7. Zhou, X.L. and Liu, J.C. (2014) Role of Notch signaling in the mammalian heart. *Braz. J. Med. Biol. Res.*, **47**, 1–10.
8. Garg, V., Muth, A.N., Ransom, J.F., Schluterman, M.K., Barnes, R., King, I.N., Grossfeld, P.D. and Srivastava, D. (2005) Mutations in NOTCH1 cause aortic valve disease. *Nature*, **437**, 270–274.
9. McBride, K.L., Riley, M.F., Zender, G.A., Fitzgerald-Butt, S.M., Towbin, J.A., Belmont, J.W. and Cole, S.E. (2008) NOTCH1 mutations in individuals with left ventricular outflow tract malformations reduce ligand-induced signaling. *Hum. Mol. Genet.*, **17**, 2886–2893.
10. Kerstjens-Frederikse, W.S., van de Laar, I.M., Vos, Y.J., Verhagen, J.M., Berger, R.M., Lichtenbelt, K.D., Klein Wassink-Ruiter, J.S., van der Zwaag, P.A., du Marchie Sarvaas, G.J., Bergman, K.A. *et al.* (2016) Cardiovascular malformations caused by NOTCH1 mutations do not keep left: data on 428 probands with left-sided CHD and their families. *Genet. Med.*, **18**, 914–923.
11. Preuss, C., Capredon, M., Wünnemann, F., Chetaille, P., Prince, A., Godard, B., Leclerc, S., Sobreira, N., Ling, H., Awadalla, P. *et al.* (2016) Family based whole exome sequencing reveals the multifaceted role of Notch Signaling in congenital heart disease. *PLoS Genet.*, **12**, e1006335.
12. Helle, E., Cordova-Palomera, A., Ojala, T., Saha, P., Potiny, P., Gustafsson, S., Ingelsson, E., Bamshad, M., Nickerson, D., Chong, J.X. *et al.* (2019) Loss of function, missense, and intronic variants in NOTCH1 confer different risks for left ventricular outflow tract obstructive heart defects in two European cohorts. *Genet. Epidemiol.*, **43**, 215–226.
13. Li, B., Yu, L., Liu, D., Yang, X., Zheng, Y., Gui, Y. and Wang, H. (2018) MIB1 mutations reduce Notch signaling activation and contribute to congenital heart disease. *Clin. Sci. (Lond)*, **132**, 2483–2491.
14. Luxán, G., Casanova, J.C., Martínez-Poveda, B., Prados, B., D'Amato, G., MacGrogan, D., González-Rajal, A., Dobarro, D., Torroja, C., Martinez, F. *et al.* (2013) Mutations in the NOTCH pathway regulator MIB1 cause left ventricular noncompaction cardiomyopathy. *Nat. Med.*, **19**, 193–201.
15. Meester, J.A.N., Sukalo, M., Schroder, K.C., Schanze, D., Baynam, G., Borck, G., Bramswig, N.C., Duman, D., Gilbert-Dussardier, B., Holder-Espinasse, M. *et al.* (2018) Elucidating the genetic architecture of Adams-Oliver syndrome in a large European cohort. *Hum. Mutat.*, **39**, 1246–1261.
16. Shi, H., O'Reilly, V.C., Moreau, J.L.M., Bewes, T.R., Yam, M.X., Chapman, B.E., Grieve, S.M., Stocker, R., Graham, R.M.,

Chapman, G. *et al.* (2016) Gestational stress induces the unfolded protein response, resulting in heart defects. *Development*, **143**, 2561–2572.
17. Sparrow, D.B., Chapman, G., Smith, A.J., Mattar, M.Z., Major, J.A., O'Reilly, V.C., Saga, Y., Alman, B.A., McGregor, L., Kageyama, R. *et al.* (2012) A mechanism for gene-environment interaction in the etiology of congenital scoliosis. *Cell*, **149**, 295–306.
18. Masek, J. and Andersson, E.R. (2017) The developmental biology of genetic Notch disorders. *Development*, **144**, 1743–1763.
19. Szot, J.O., Cuny, H., Blue, G.M., Humphreys, D.T., Ip, E., Harrison, K., Sholler, G.F., Giannoulatou, E., Leo, P., Duncan, E.L. *et al.* (2018) A screening approach to identify clinically actionable variants causing congenital heart disease in exome data. *Circ. Genom. Precis. Med.*, **11**, e001978.
20. Lacaze, P., Pinese, M., Kaplan, W., Stone, A., Brion, M.J., Woods, R.L., McNamara, M., McNeil, J.J., Dinger, M.E. and Thomas, D.M. (2019) The medical genome reference Bank: a whole-genome data resource of 4000 healthy elderly individuals. Rationale and cohort design. *Eur. J. Hum. Genet.*, **27**, 308–316.
21. Meester, J.A., Southgate, L., Stittrich, A.B., Venselaar, H., Beekmans, S.J., den Hollander, N., Bijlsma, E.K., Helderman-van den Enden, A., Verheij, J.B., Glusman, G. *et al.* (2015) Heterozygous loss-of-function mutations in DLL4 cause Adams-Oliver syndrome. *Am. J. Hum. Genet.*, **97**, 475–482.
22. Sparrow, D.B., Chapman, G., Wouters, M.A., Whittock, N.V., Ellard, S., Fatkin, D., Turnpenny, P.D., Kusumi, K., Sillence, D. and Dunwoodie, S.L. (2006) Mutation of the LUNATIC FRINGE gene in humans causes spondylocostal dysostosis with a severe vertebral phenotype. *Am. J. Hum. Genet.*, **78**, 28–37.
23. Hoyne, G.F., Chapman, G., Sontani, Y., Pursglove, S.E. and Dunwoodie, S.L. (2011) A cell autonomous role for the Notch ligand Delta-like 3 in $\alpha\beta$ T-cell development. *Immunol. Cell Biol.*, **89**, 696–705.
24. Vardar, D., North, C.L., Sanchez-Irizarry, C., Aster, J.C. and Blacklow, S.C. (2003) Nuclear magnetic resonance structure of a prototype Lin12-Notch repeat module from human Notch1. *Biochemistry*, **42**, 7061–7067.
25. Sanchez-Irizarry, C., Sanchez-Irizarry, C., Carpenter, A., Carpenter, A.C., Weng, A., Weng, A.P., Pear, W.S., Pear, W., Aster, J.C., Aster, J. *et al.* (2004) Notch subunit heterodimerization and prevention of ligand-independent Proteolytic activation depend, respectively, on a novel domain and the LNR repeats. *Mol. Cell. Biol.*, **24**, 9265–9273.
26. Gordon, W.R., Vardar-Ulu, D., Histen, G., Sanchez-Irizarry, C., Aster, J.C. and Blacklow, S.C. (2007) Structural basis for autoinhibition of Notch. *Nat. Struct. Mol. Biol.*, **14**, 295–300.
27. Logeat, F., Bessia, C., Brou, C., LeBail, O., Jarriault, S., Seidah, N.G. and Israël, A. (1998) The Notch1 receptor is cleaved constitutively by a furin-like convertase. *Proc. Natl. Acad. Sci. USA*, **95**, 8108–8112.
28. Blaumueller, C.M., Qi, H., Zagouras, P. and Artavanis-Tsakonas, S. (1997) Intracellular cleavage of Notch leads to a heterodimeric receptor on the plasma membrane. *Cell*, **90**, 281–291.
29. Nichols, J.T., Miyamoto, A., Olsen, S.L., D'Souza, B., Yao, C. and Weinmaster, G. (2007) DSL ligand endocytosis physically dissociates Notch1 heterodimers before activating proteolysis can occur. *J. Cell Biol.*, **176**, 445–458.
30. Gordon, W.R., Vardar-Ulu, D., L'Heureux, S., Ashworth, T., Malecki, M.J., Sanchez-Irizarry, C., McArthur, D.G., Histen, G., Mitchell, J.L., Aster, J.C. *et al.* (2009) Effects of S1 cleavage on the structure, surface export, and signaling activity of human Notch1 and Notch2. *PLoS One*, **4**, e6613.
31. Ritchie, H.E., Ababneh, D.H., Oakes, D.J., Power, C.A. and Webster, W.S. (2013) The teratogenic effect of dofetilide during rat limb development and association with drug-induced bradycardia and hypoxia in the embryo. *Birth Defects Res. B Dev. Reprod. Toxicol.*, **98**, 144–153.
32. Halin, C., Tobler, N.E., Vigl, B., Brown, L.F. and Detmar, M. (2007) VEGF-A produced by chronically inflamed tissue induces lymphangiogenesis in draining lymph nodes. *Blood*, **110**, 3158–3167.
33. Hallmann, R., Mayer, D.N., Berg, E.L., Broermann, R. and Butcher, E.C. (1995) Novel mouse endothelial cell surface marker is suppressed during differentiation of the blood brain barrier. *Dev. Dyn.*, **202**, 325–332.
34. Page, D.J., Miossec, M.J., Williams, S.G., Monaghan, R.M., Fotiou, E., Cordell, H.J., Sutcliffe, L., Topf, A., Bourgey, M., Bourque, G. *et al.* (2019) Whole exome sequencing reveals the major genetic contributors to nonsyndromic tetralogy of Fallot. *Circ. Res.*, **124**, 553–563.
35. Lin, A.E., Westgate, M.N., van der, M.E., Lacro, R.V. and Holmes, L.B. (1998) Adams-Oliver syndrome associated with cardiovascular malformations. *Clin. Dysmorphol.*, **7**, 235–241.
36. Algaze, C., Esplin, E.D., Lowenthal, A., Hudgins, L., Tacy, T.A. and Selamet Tierney, E.S. (2013) Expanding the phenotype of cardiovascular malformations in Adams-Oliver syndrome. *Am. J. Med. Genet. A*, **161A**, 1386–1389.
37. Andrawes, M.B., Xu, X., Liu, H., Ficarro, S.B., Marto, J.A., Aster, J.C. and Blacklow, S.C. (2013) Intrinsic selectivity of Notch 1 for Delta-like 4 over Delta-like 1. *J. Biol. Chem.*, **288**, 25477–25489.
38. Luca, V.C., Jude, K.M., Pierce, N.W., Nachury, M.V., Fischer, S. and Garcia, K.C. (2015) Structural basis for Notch1 engagement of Delta-like 4. *Science*, **347**, 847–853.
39. Acar, M., Jafar-Nejad, H., Takeuchi, H., Rajan, A., Ibrani, D., Rana, N.A., Pan, H., Haltiwanger, R.S. and Bellen, H.J. (2008) Rumi is a CAP10 domain glycosyltransferase that modifies Notch and is required for Notch signaling. *Cell*, **132**, 247–258.
40. Aminkeng, F. (2015) DLL4 loss-of-function heterozygous mutations cause Adams-Oliver syndrome. *Clin. Genet.*, **88**, 532–532.
41. Nagasaka, M., Taniguchi-Ikeda, M., Inagaki, H., Ouchi, Y., Kurokawa, D., Yamana, K., Harada, R., Nozu, K., Sakai, Y., Mishra, S.K. *et al.* (2017) Novel missense mutation in DLL4 in a Japanese sporadic case of Adams-Oliver syndrome. *J. Hum. Genet.*, **62**, 851–855.
42. Gallo Llorente, L., Luther, H., Schneppenheim, R., Zimmermann, M., Felice, M. and Horstmann, M.A. (2014) Identification of novel NOTCH1 mutations: increasing our knowledge of the NOTCH signaling pathway. *Pediatr. Blood Cancer*, **61**, 788–796.
43. Southgate, L., Sukalo, M., Karountzos, A.S.V., Taylor, E.J., Collinson, C.S., Ruddy, D., Snape, K.M., Dallapiccola, B., Tolmie, J.L., Joss, S. *et al.* (2015) Haploinsufficiency of the NOTCH1 receptor as a cause of Adams–Oliver syndrome with variable cardiac anomalies. *Circ. Cardiovasc. Genet.*, **8**, 572–581.
44. Stittrich, A.B., Lehman, A., Bodian, D.L., Ashworth, J., Zong, Z., Li, H., Lam, P., Khromykh, A., Iyer, R.K., Vockley, J.G. *et al.* (2014) Mutations in NOTCH1 cause Adams-Oliver syndrome. *Am. J. Hum. Genet.*, **95**, 275–284.
45. Yeo, G. and Burge, C.B. (2004) Maximum entropy modeling of short sequence motifs with applications to RNA splicing signals. *J. Comput. Biol.*, **11**, 377–394.

46. Greenway, S.C., Pereira, A.C., Lin, J.C., DePalma, S.R., Israel, S.J., Mesquita, S.M., Ergul, E., Conta, J.H., Korn, J.M., McCarroll, S.A. *et al*. (2009) De novo copy number variants identify new genes and loci in isolated sporadic tetralogy of Fallot. *Nat. Genet*., **41**, 931–935.
47. Diez, H., Fischer, A., Winkler, A., Hu, C.-J., Hatzopoulos, A.K., Breier, G. and Gessler, M. (2007) Hypoxia-mediated activation of Dll4-Notch-Hey2 signaling in endothelial progenitor cells and adoption of arterial cell fate. *Exp. Cell Res*., **313**, 1–9.
48. Landor, S.K.-J. and Lendahl, U. (2017) The interplay between the cellular hypoxic response and Notch signaling. *Exp. Cell Res*., **356**, 146–151.
49. Nus, M., MacGrogan, D., Martínez-Poveda, B., Benito, Y., Casanova, J.C., Fernández-Avilés, F., Bermejo, J. and de la Pompa, J.L. (2011) Diet-induced aortic valve disease in mice haploinsufficient for the Notch pathway effector RBPJK/CSL. *Arterioscler. Thromb. Vasc. Biol*., **31**, 1580–1588.
50. Basu, M., Zhu, J.-Y., LaHaye, S., Majumdar, U., Jiao, K., Han, Z. and Garg, V. (2017) Epigenetic mechanisms underlying maternal diabetes-associated risk of congenital heart disease. *JCI Insight*, **2**, 1–20.
51. Patel, S.S. and Burns, T.L. (2013) Nongenetic risk factors and congenital heart defects. *Pediatr. Cardiol*., **34**, 1535–1555.
52. Øyen, N., Diaz, L.J., Leirgul, E., Boyd, H.A., Priest, J., Mathiesen, E.R., Quertermous, T., Wohlfahrt, J. and Melbye, M. (2016) Prepregnancy diabetes and offspring risk of congenital heart disease. *Circulation*, **133**, 2219–2221.
53. Watkins, M.L., Rasmussen, S.A., Honein, M.A., Botto, L.D. and Moore, C.A. (2003) Maternal obesity and risk for birth defects. *Pediatrics*, **111**, 1152–1158.
54. Jenkins, K.J., Correa, A., Feinstein, J.A., Botto, L., Britt, A.E., Daniels, S.R., Elixson, M., Warnes, C.A. and Webb, C.L. (2007) Noninherited risk factors and congenital cardiovascular defects: current knowledge. *Circulation*, **115**, 2995–3014.
55. Zheng, J.Y., Tian, H.T., Zhu, Z.M., Li, B., Han, L., Jiang, S.L., Chen, Y., Li, D.T., He, J.C., Zhao, Z. *et al*. (2013) Prevalence of symptomatic congenital heart disease in Tibetan school children. *Am. J. Cardiol*., **112**, 1468–1470.
56. Webster, W.S., Nilsson, M. and Ritchie, H. (2014) Therapeutic drugs that slow the heart rate of early rat embryos. Is there a risk for the human? *Curr. Pharm. Des*., **20**, 5364–5376.
57. Sullivan, P.M., Dervan, L.A., Reiger, S., Buddhe, S. and Schwartz, S.M. (2015) Risk of congenital heart defects in the offspring of smoking mothers: a population-based study. *J. Pediatr*., **166**, 978, e972–984.
58. Ramakrishnan, A., Lee, L.J., Mitchell, L.E. and Agopian, A.J. (2015) Maternal hypertension during pregnancy and the risk of congenital heart defects in offspring: a systematic review and meta-analysis. *Pediatr. Cardiol*., **36**, 1442–1451.
59. Ornoy, A., Reece, E.A., Pavlinkova, G., Kappen, C. and Miller, R.K. (2015) Effect of maternal diabetes on the embryo, fetus, and children: congenital anomalies, genetic and epigenetic changes and developmental outcomes. *Birth Defects Res. C Embryo Today*, **105**, 53–72.
60. Vandenberg, J.I., Perry, M.D., Perrin, M.J., Mann, S.A., Ke, Y. and Hill, A.P. (2012) hERG K(+) channels: structure, function, and clinical significance. *Physiol. Rev*., **92**, 1393–1478.
61. Li, H. (2012) Exploring single-sample SNP and INDEL calling with whole-genome de novo assembly. *Bioinformatics*, **28**, 1838–1844.
62. Van der Auwera, G.A., Carneiro, M.O., Hartl, C., Poplin, R., Del Angel, G., Levy-Moonshine, A., Jordan, T., Shakir, K., Roazen, D., Thibault, J. *et al*. (2013) From FastQ data to high confidence variant calls: the genome analysis toolkit best practices pipeline. *Curr. Protoc. Bioinformatics*, **43**, 11-10–11-33.
63. Arthur, R., Schulz-Trieglaff, O., Cox, A.J. and O'Connell, J. (2017) AKT: ancestry and kinship toolkit. *Bioinformatics*, **33**, 142–144.
64. Purcell, S.M., Moran, J.L., Fromer, M., Ruderfer, D., Solovieff, N., Roussos, P., O'Dushlaine, C., Chambert, K., Bergen, S.E., Kähler, A. *et al*. (2014) A polygenic burden of rare disruptive mutations in schizophrenia. *Nature*, **506**, 185–190.
65. Lee, S., Emond, M.J., Bamshad, M.J., Barnes, K.C., Rieder, M.J., Nickerson, D.A., Team, N.G.E.S.P.-E.L.P., Christiani, D.C., Wurfel, M.M. and Lin, X. (2012) Optimal unified approach for rare-variant association testing with application to small-sample case-control whole-exome sequencing studies. *Am. J. Hum. Genet*., **91**, 224–237.
66. Richards, S., Aziz, N., Bale, S., Bick, D., Das, S., Gastier-Foster, J., Grody, W.W., Hegde, M., Lyon, E., Spector, E. *et al*. (2015) Standards and guidelines for the interpretation of sequence variants: a joint consensus recommendation of the American College of Medical Genetics and Genomics and the Association for Molecular Pathology. *Genet. Med*., **17**, 405–423.
67. Li, Q. and Wang, K. (2017) InterVar: clinical interpretation of genetic variants by the 2015 ACMG-AMP guidelines. *Am. J. Hum. Genet*., **100**, 267–280.
68. James, A.C., Szot, J.O., Iyer, K., Major, J.A., Pursglove, S.E., Chapman, G. and Dunwoodie, S.L. (2014) Notch4 reveals a novel mechanism regulating Notch signal transduction. *Biochim. Biophys. Acta*., **1843**, 1272–1284.
69. Chapman, G., Major, J.A., Iyer, K., James, A.C., Pursglove, S.E., Moreau, J.L. and Dunwoodie, S.L. (2016) Notch1 endocytosis is induced by ligand and is required for signal transduction. *Biochim. Biophys. Acta*., **1863**, 166–177.
70. Moreau, J.L., Artap, S.T., Shi, H., Chapman, G., Leone, G., Sparrow, D.B. and Dunwoodie, S.L. (2014) Cited2 is required in trophoblasts for correct placental capillary patterning. *Dev. Biol*., **392**, 62–79.
71. Chapman, G., Sparrow, D.B., Kremmer, E. and Dunwoodie, S.L. (2011) Notch inhibition by the ligand Delta-like 3 defines the mechanism of abnormal vertebral segmentation in spondylocostal dysostosis. *Hum. Mol. Genet*., **20**, 905–916.
72. Yang, X., Klein, R., Tian, X., Cheng, H.T., Kopan, R. and Shen, J. (2004) Notch activation induces apoptosis in neural progenitor cells through a p53-dependent pathway. *Dev. Biol*., **269**, 81–94.
73. O'Reilly, V.C., Lopes Floro, K., Shi, H., Chapman, B.E., Preis, J.I., James, A.C., Chapman, G., Harvey, R.P., Johnson, R.S., Grieve, S.M. *et al*. (2014) Gene-environment interaction demonstrates the vulnerability of the embryonic heart. *Dev. Biol*., **391**, 99–110.